Effects of a one-dimensional surface defect on designer surface plasmon polaritons*

Ding Lan(丁 岚), Liu Jin-Song(刘劲松)†, and Wang Ke-Jia(王可嘉)

Wuhan National Laboratory for Optoelectronics, School of Optoelectronic Science and Engineering, Huazhong University of Science and Technology, Wuhan 430074, *China*

(Received 6 February 2010; revised manuscript received 6 April 2010)

By using a finite difference time domain (FDTD) method, the effects of a one-dimensional (1D) surface defect on designer surface plasmon polaritons (designer SPPs) supported by a 1D metallic grating in THz domain are investigated. When the size of the defect is in a special range which is not too large, the designer SPPs reflected and scattered by the defect are weak enough to be neglected. The defect only induces a disturbance in the energy distribution of the designer SPP supported by the whole defect grating. If the defect size exceeds the said range, the reflecting and scattering are dominant in the influences of the defect on designer SPPs. Our analysis opens opportunities to control and direct designer SPPs by introducing a 1D defect, especially in low frequency domain.

Keywords: surface states, surface plasmons, electromagnetic theory, grating

PACC: 7320J, 7320M, 4110H, 4280F

1. Introduction

Surface plasmon polaritons (SPPs) are electromagnetic (EM) waves bound to a dielectric-metal interface and caused by the surface oscillations of the electron plasma of the metal.[1,2] Their unique optical properties have, among other applications, the potential for designing highly integrated photonic circuits with length scales much smaller than those currently achieved.[3] There have been several theoretical studies of the scattering or reflecting of SPPs by isolated or periodic defects of various types on an otherwise planar metal surface,[4−9] as well as several experimental studies of such scattering or reflecting processes.[10−12] These works have shown evidence of drastically distinct effects of surface defect size on SPPs. Specifically, surface defects favouring SPP reflection and light coupling, called SPP mirrors and light emitters,[5,6] have been described respectively. However, the studies mentioned above have not taken low frequency regime (such as THz regime and microwave regime) into account, in which metals can be regarded as perfect electrical conductors (PECs), and SPPs are highly delocalized. Pendry and co-workers have shown that bound electromagnetic surface waves mimicking SPPs, namely spoof SPPs, can be sustained even by a PEC, provided that its surface is periodically corrugated.[13] If the size and spacing of the corrugations is much smaller than the wavelength, the electromagnetic response of the surface can be described as an effective medium, and the dispersion relation of spoof SPPs can be engineered via the geometry of the surface,[13,14] thus spoof SPPs has a name of designer SPPs. The existence of designer SPPs was indirectly verified by microwave reflectivity measurements.[15] It was believed that a measured enhanced transmission phenomenon at THz regime should originate from the crucial contribution of designer SPPs.[16] Designer SPPs propagation on structured metal surfaces was directly observed and the results were quantitatively consistent with theoretical predictions.[17] The designer SPP theory was also used to study the slow-light characteristics of structured metal surfaces with a one-dimensional graded grating of varying depth in THz domain.[18] Recently, a method to design transmission resonances through subwavelength apertures based on designer SPPs was proposed in THz regime.[19] However, in previous works, little attention has been paid on the effects of surface defects on designer SPPs.

Designer SPPs promise the ability to engineer surface EM modes on structured metal surfaces at low frequency regime. This property allows us to actively design some relevant experiments, such as microwave re-

*Project supported by the National Natural Science Foundation of China (Grant No. 10974063), the Research Foundation of Wuhan National Laboratory (Grant No. P080008), and the National Basic Research Program of China (Grant No. 2007CB310403).

†Corresponding author. E-mail: jsliu4508@vip.sina.com

© 2010 Chinese Physical Society and IOP Publishing Ltd

flectivity measurements[15] and highly confined guiding THz surface wave.[17] However, to actively design periodically corrugated surfaces with some structure defects, which may lead to designer SPP reflection and coupling, has not been considered so far. In this paper, by using finite difference time domain (FDTD) method[20] we investigate the effects of a one-dimensional (1D) surface defect on designer SPPs, which is supported by a 1D metallic grating in THz domain. Results show that when the size of the defect is small enough, the defect only induces a disturbance in the energy distribution of the designer SPP that is supported by the whole defect grating. If the size exceeds the said range, the reflecting and scattering are dominant in the effects of the defect on designer SPPs. These results allow us to control and direct designer SPPs by introducing a 1D surface defect.

2. Model and method

First, we pay our attention to a uniform 1D metallic grating, which consists of an array of 1D grooves formed just beneath the metallic surface, with depth h, width d, and lattice constant p (see the inset to Fig. 1(a)). For such a structure, if $d < p \ll \lambda_0$, where λ_0 is the wavelength of radiation, externally incident radiation is insensitive to the details of the grooves. In most previous works of SPPs in metallic structures for THz domain, the metals were treated as PECs.[13,18] Under these assumptions, by employing the designer SPP theory, the dispersion relation for transverse magnetic (TM) waves (E_x, E_z and H_y) propagating in the z direction can be obtained[13,14,18] as follows:

$$\frac{d}{p}\sum_{n=-\infty}^{+\infty}\frac{1}{\tau_n h}\left[\frac{\sin(\beta_n d/2)}{\beta_n d/2}\right]^2=\frac{\cot k_0 h}{k_0 h}, \qquad (1)$$

where β is the propagation constant, $\beta_n=\beta+2\pi n/p$, τ_n is the exponential decay factor, $\beta_n^2-\tau_n^2=k_0^2=\omega^2\mu_0\varepsilon_0$, and ε_0 and μ_0 are the permittivity and permeability in vacuum. Figure 1(a) shows the dispersion relation calculated for $h=70$ μm, $d=20$ μm, and $p=50$ μm, which are suggested in Ref. [21]. The same dispersion relation could also be obtained by replacing the array of grooves by an effective medium with effective permittivity and effective permeability.[14] In other words, the effective medium can support designer SPPs when the frequency of incident wave f is below the cutoff frequency f_c, which is obtained from the dispersion relation. Moreover, if the frequency of incident wave approaches f_c, the electromagnetic energy will be confined tightly near the grating surface, as shown in Fig. 2(a). Note that in our work we paid close attention on designer SPPs in region I as illustrated in the inset to Fig. 1(a), in which structure defect would mainly influence on designer SPPs.

In order to investigate the effects of a 1D surface defect on designer SPPs, we introduce a size defect in the metallic grating mentioned above at the position of $z=+60$ μm. One can see from Fig. 1(b) that the defect is a grating protuberance with changing height $h+\Delta h$ or changing width $a+\Delta a$, where $a=p-d$. In our model, the electric intensities of designer SPPs in region I are considered respectively in the following three parts: the vicinity of the defect (region D), and

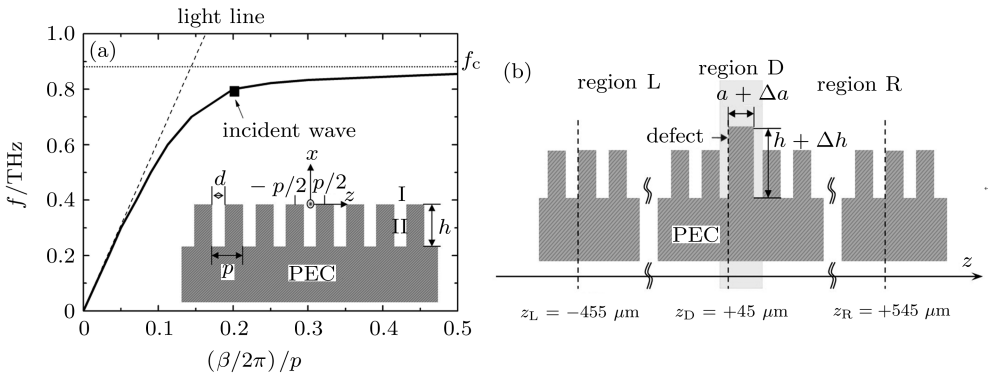


Fig. 1. (a) Dispersion curve calculated for the uniform grating with $h=70$ μm, $d=20$ μm, and $p=50$ μm, where β is the propagation constant in z direction. Inset: A model of uniform 1D metallic grating with depth h, width d, and lattice constant p. (b) A grating with the same parameters illustrated in (a) has a defect with changing height $h+\Delta h$ or changing width $a+\Delta a$.

the regions to the left (region L) and right (region R) of the defect. By using a two-dimensional (2D) FDTD simulation tool,[20] namely Fullwave 3.0.1, we simulated the process of designer SPPs propagating along the defect grating. We have assumed the depth h, width d, and lattice constant p of the defect grating to be 70, 20, and 50 μm, respectively. The simulation region has dimensions of 2100 μm$\times$400 μm, and it is surrounded by a perfectly matched layer absorber. A uniform cell dimension of $\Delta x = 2$ μm and $\Delta z = 2$ μm is employed. The total length L of the grating is set to 2000 μm, and the calculation time t_c is approximately 65536 μm/c_0. It is enough for steady-state designer SPPs propagating from the left-hand side to the right-hand side of the simulation region within the calculation time. Under these assumptions, we set the frequency of the incident TM wave to 0.8 THz (375 μm), which is close to the cutoff frequency f_c shown in Fig. 1(a).

3. Numerical results and discussion

The 0.8-THz TM wave with power of 0.1 a.u. is incoming from the left-hand side of the simulation region. Note that the electric intensity distribution for the uniform/defect grating was obtained at the plane of 10 μm above the metallic surface, as illustrated in Fig. 2(a). Figure 2(b) shows the electric intensity distributions for the uniform grating (thin solid line) displayed in Fig. 1(a), and for defect gratings with $\Delta h = 30$ μm, $\Delta a = 0$ (thick solid line) and $\Delta h = 0$, $\Delta a = 30$ μm (dashed line), respectively. One can see from Fig. 2(b) that each of the distributions consists of many electric intensity peaks, which can be described by their locations (z_p) and magnitude ($|\boldsymbol{E}|_p^2$). These regularly spaced peaks in field intensity across the z direction of the structure are caused by the accumulated charge near the grating ridge corners, which were mentioned in Ref. [22] and investigated thoroughly in Ref. [23]. It is clear that the distance between two adjacent peaks in each distribution is relatively unchanging. Moreover, for each distribution, the difference of $|\boldsymbol{E}|_p^2$ between any two electric intensity peaks, which are located in each of regions L and R, is very small. Otherwise, there is only one electric intensity peak in region D, thus the characteristics of the electric intensity in region D can be directly represented by z_p and $|\boldsymbol{E}|_p^2$ of this peak, which is around z_D. Based on these findings, we pay our attention on three electric intensity peaks, which are at or near $z_L = -455$ μm, $z_R = +545$ μm and $z_D = +45$ μm, as shown in Fig. 1(b) and Fig. 2. The changes of z_p and $|\boldsymbol{E}|_p^2$ of these three peaks can represent the defect size dependence of the electric intensity distributions for region L, region R and region D, respectively. For simplicity, the locations of z_L, z_R, and z_D, at which these three peaks for the uniform grating are located, are taken as reference positions. Then the change of z_p corresponding to each of the three peaks can be described by the peak position variation Δz_p, where Δz_p is determined by $z_p - z_{L/R/D}$.

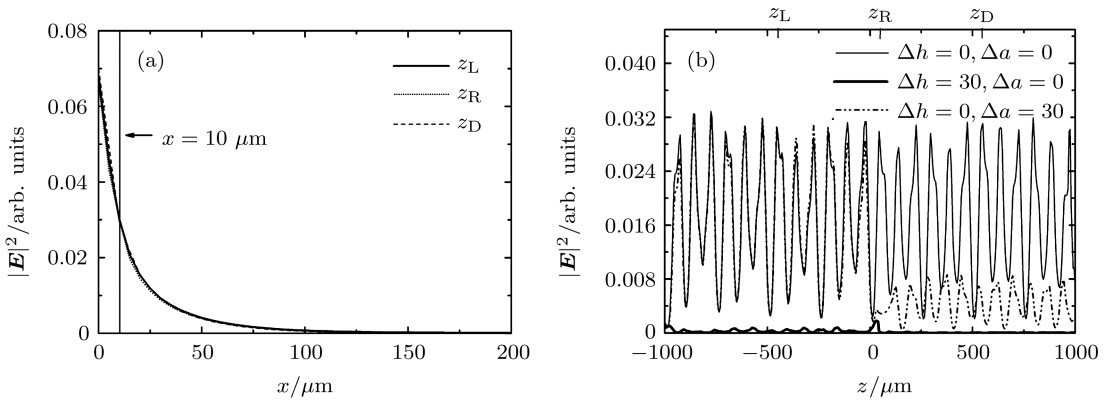


Fig. 2. (a) The electric intensity versus distance from the metallic surface at z_L, z_R and z_D for the uniform grating with $h = 70$ μm, $d = 20$ μm, and $p = 50$ μm. (b) The electric intensity distributions for the uniform grating (black solid line) displayed in Fig. 1(a), and for defect gratings with $\Delta h = 30$ μm, $\Delta a = 0$ (solid line) and $\Delta h = 0$, $\Delta a = 30$ μm (dashed line).

We first consider the effect of defect height variation Δh on designer SPPs. Thus, the width variation Δa is fixed at 0. Figure 3 shows the defect height variation dependence of the magnitude and position variation of

the three electric intensity peaks, which are near $z_{\rm L}$, $z_{\rm R}$ and $z_{\rm D}$ respectively. Note that Δh increases by steps of 5 μm from -70 μm to 40 μm in Fig. 3. Specifically, $\Delta h = -70$ μm corresponds to the situation that the grating ridge at $z = +60$ μm is missing.

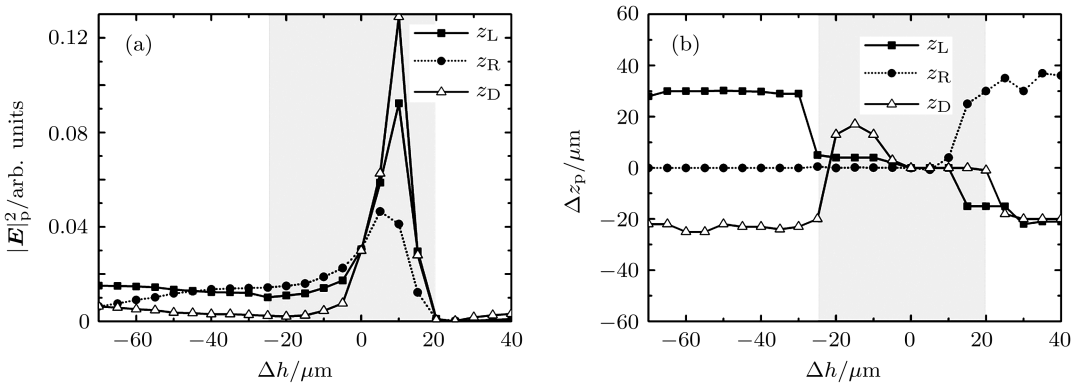


Fig. 3. The defect height variation (Δh) dependence of (a) magnitude and (b) position variation of the electric intensity peaks around $z_{\rm L} = -455$ μm, $z_{\rm R} = +545$ μm, and $z_{\rm D} = +45$ μm.

When Δh is in the range of -25 μm to 20 μm, the variation tendencies of $|\boldsymbol{E}|_{\rm p}^2$ for $z_{\rm L}$ and $z_{\rm R}$ are similar, while both of the peak position variations for $z_{\rm L}$ and $z_{\rm R}$ are nearly zero, as shown in Figs. 3(a) and 3(b). It means that the defect height variation dependence of the electric intensity distributions for regions L and R resembles each other. Generally, due to the effects of SPP reflecting and scattering by defect, the variation tendencies of the electric intensity magnitude for region L and R may not be similar[6] unless the energy reflected and scattered by the defect is very weak. Thus, the influence of reflecting and scattering by the defect on designer SPPs can be neglected in the range of -25 μm$< \Delta h < 20$ μm. Figures 3(a) and 3(b) also show that $|\boldsymbol{E}|_{\rm p}^2$ and $\Delta z_{\rm p}$ for region D change more dramatically with Δh and the defect size dependence of them is different from that for regions L and R. These results indicate that the defect grating responses to the incident EM wave as a whole, and the structure defect only induces a disturbance in the electric intensity distribution in region D. In other words, the designer SPP state, whose energy distribution has a defect in region D, is supported by the whole grating, when Δh is small enough.

In the range of $\Delta h < -25$ μm, figure 3(a) shows that $|\boldsymbol{E}|_{\rm p}^2$ for $z_{\rm L}$ slightly increases and $|\boldsymbol{E}|_{\rm p}^2$ for $z_{\rm R}$ decreases with increasing $|\Delta h|$, which represents that the variation tendencies of the electric intensity magnitude for regions L and R are opposite. Thus, reflecting and scattering of designer SPPs are dominant in the effects of the defect on designer SPPs. According to Fig. 3(a), it is reasonable to infer that the designer SPP reflection coefficient slightly increases with increasing $|\Delta h|$ while the transmission coefficient slightly decreases, which is similar to the real situation of SPPs.[6] Figure 3(a) also shows that $|\boldsymbol{E}|_{\rm p}^2$ for region D approaches 0.006 and changes very slowly with increasing $|\Delta h|$. It means that the energy of the designer SPPs, which are scattered to the upside of the defect, is not sensitive to the change of Δh, when Δh is less than -25 μm. On the other hand, the electric intensity peak positions for regions L and D change from 0 to $+30$ μm and -20 μm, respectively, when $\Delta h < -25$ μm. It means that the position where the accumulated charge is located moves to the other corner of the same grating ridge (for $\Delta z_{\rm p} = +30$ μm) and the corner of the adjacent ridge (for $\Delta z_{\rm p} = -20$ μm), which can be easily deduced from Fig. 3(b). Specifically, if Δh is larger than 25 μm, the energy of transmitted and reflected designer SPP is very weak, as shown in Fig. 3(a). The transmission and reflection ability of designer SPPs is poorer than that of real SPPs when the defect height is rather large. Moreover, in the range of $\Delta h > 20$ μm, one can deduce from Fig. 3(b) that the positions of the electric intensity peaks in regions L and D move about -20 μm, while that of region R changes about $+30$ μm. The reason for these peak position movements are similar to the situation of $\Delta h < -25$ μm. These characteristics allow us to control the distribution of electric intensity along the defect grating.

We then consider the influence of defect width variation Δa on designer surface plasmon polaritons, while the height variation Δh is set to 0. Figure 4 illustrates the defect width variation dependence of the magnitude and position variation of the three electric intensity peaks, which are around $z_{\rm L}$, $z_{\rm R}$ and $z_{\rm D}$. For real surface plasmon polaritons, $\Delta h = 0$ means that

there is no defect on the metal surface. However, since the designer surface plasmon polaritons are supported by an array of subwavelength grooves, it is very different that the defect still has influences on designer surface plasmon polaritons with $\Delta h = 0$ and $\Delta a \neq 0$. Notice that Δa changes from -25 μm to 40 μm by steps of 5 μm in Fig. 4, and $\Delta a = 40$ μm is the largest width of the isolated defect in the grating.

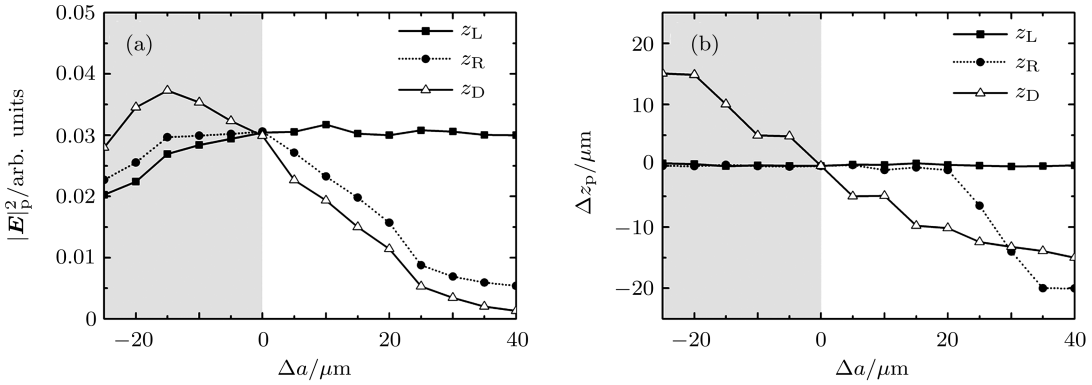


Fig. 4. The defect width variation (Δa) dependence of (a) magnitude and (b) position variation of the electric intensity peaks around $z_{\rm L} = -455$ μm, $z_{\rm R} = +545$ μm, and $z_{\rm D} = +45$ μm.

As the defect width Δa is in the -20 μm to 0 range, one can see from Figs. 4(a) and 4(b) that the variation tendencies of $|\boldsymbol{E}|_{\rm p}^2$ for $z_{\rm L}$ and $z_{\rm R}$ are similar, and both of the peak position variations for them are nearly zero. These characteristics resemble those of -25 μm$< \Delta h < 20$ μm. Thus, the energy of designer SPPs reflected and scattered by the defect is weak enough to be neglected. Furthermore, figure 4 renders that $|\boldsymbol{E}|_{\rm p}^2$ and $\Delta z_{\rm p}$ for region D are sensitive to the change of Δa, which is similar to the situation of -25 μm$< \Delta h < 20$ μm. These results show that the designer SPP state is supported by the whole grating, whose energy distribution only has a disturbance in the vicinity of the defect, but the disturbance is weaker than that for -25 μm$< \Delta h < 20$ μm.

When Δa is larger than 0, the results shown in Fig. 4 can be compared with those of Fig. 3 in the range of $\Delta h < -25$ μm. We can infer from Fig. 4 that reflecting and scattering are the main effects of the defect on the designer SPPs. The transmission coefficient decreases with increasing $|\Delta a|$, which is also similar to real SPPs when Δh is not zero. Since the position where the accumulated charge is located moves to the corner of the adjacent grating ridge, the intensity peak position of the transmitted designer SPPs changes about -20 μm when Δa is larger than 0. Notice that $|\boldsymbol{E}|_{\rm p}^2$ and $\Delta z_{\rm p}$ for $z_{\rm L}$ hardly change with increasing $|\Delta a|$, which is different from the situation of $\Delta h < -25$ μm. These results imply that the defect mainly works influence on the transmitted designer SPPs.

Finally, it is necessary to have a further discussion based on these results. Compared with the incident wavelength (λ_0) 375 μm, -25 μm$< \Delta h < 20$ μm and -25 μm$< \Delta a < 0$ are corresponding to $-0.067\lambda_0 < \Delta h < 0.053\lambda_0$ and $-0.067\lambda_0 < \Delta a < 0$, respectively. For the situation of $\Delta a = 0$ and $-0.067\lambda_0 < \Delta h < 0.053\lambda_0$, the defect grating responses to the incident EM wave as a whole, and the designer SPP state, whose energy distribution has a disturbance in region D, is supported by the whole grating. If the defect height variation exceeds this range, reflecting and scattering are dominant in the effects of the defect on designer SPPs. On the other hand, for $\Delta h = 0$ and $-0.067\lambda_0 < \Delta a < 0$, the situation resembles that of $-0.067\lambda_0 < \Delta h < 0.053\lambda_0$, although the disturbance is weaker. When Δa exceeds this range, the results resemble those of $\Delta h < -0.067\lambda_0$ or $\Delta h > 0.053\lambda_0$, but the defect mainly has influence on the transmitted designer SPPs. Based on these findings, by introducing a defect, we can actively design the energy distribution of designer SPPs propagating on a grating. For example, if we set Δa and Δh to 0 and 10 μm respectively, more energy will be localized at the defect, as shown in Fig. 3. This characteristic may be used in the coupling between designer SPPs and external field. Moreover, a kind of designer SPP attenuator can be obtained when $\Delta h = 0$ and Δa is larger than 0. These examples mean that designer SPPs can be controlled actively by an appropriate defect grating integrated on a chip.

4. Conclusion

In this article the effects of a 1D surface defect on designer SPPs are discussed in detail. When the defect size is small enough, the defect only induces a disturbance in the energy distribution of the designer SPP supported by the whole grating, and the reflecting and scattering can be neglected. If the defect size exceeds the said range, the reflecting and scattering are dominant in the influences of the defect on designer SPPs. Our analysis opens opportunities to control and direct designer SPPs by introducing a 1D defect, especially in THz to microwave regimes. Such a feature could realize novel applications such as devices integrated on a chip for controlling the energy distribution of surface waves. However, further theoretical work is needed to thoroughly explain the effects of 1D or 2D defects on designer SPPs. We also expect experimental work to demonstrate our results.

References

[1] Agranovich V M and Mills D L 1982 *Surface Polaritons* (Amsterdam: North-Holland)

[2] Raether H 1988 *Surface Polaritons on Smooth and Rough Surfaces and on Gratings* (Berlin: Springer)

[3] de León-Pérez F, Brucoli G, García-Vidal F J and Martín-Moreno L 2008 *New J. Phys.* **10** 1

[4] Pincemin F, Maradudin A A, Boardman A D and Greffet J J 1994 *Phys. Rev.* B **50** 15261

[5] S'a nchez-Gil J A 1998 *Appl. Phys. Lett.* **73** 3509

[6] S'anchez-Gil J A and Maradudin A A 1999 *Phys. Rev.* B **60** 8359

[7] S'anchez-Gil J A and Maradudin A A 2004 *Opt. Express* **12** 883

[8] Haitao Liu, Philippe Lalanne, Xiaoyan Yang and Jean-Paul Hugonin 2008 *IEEE Journal of Selected Topics in Quantum Electronics* **14** 1522

[9] Wang L C, Deng L, Cui N, Niu Y P and Gong S Q 2010 *Chin. Phys.* B **19** 017303

[10] Rothenhäausler B and Knoll W 1987 *Appl. Phys. Lett.* **51** 783

[11] Berger C E H, Koioyman R P H and Greve J 1999 *Opt. Commun.* **167** 183

[12] Smolyaninov I I, Mazzoni D L, Mait J and Davis C C 1997 *Phys. Rev.* B **56** 1601

[13] Pendry J B, Martin-Moreno L and Garcia-Vidal F J 2004 *Science* **305** 847

[14] Garcia-Vidal F J, Martin-Moreno L and Pendry J B 2005 *J. Opt.* A **7** S97

[15] Hibbins A P, Evans B R and Sambles J R 2005 *Science* **308** 670

[16] Tanaka M, Miyamaru F, Hangyo M, Tanaka T, Akazawa M and Sano E 2005 *Opt. Lett.* **30** 1210

[17] Williams C R, Andrews S R, Maier S A, FernÃndez-DomÃnguez, MartÃn-Moreno L and Garcia-Vidal F J 2008 *Nature Photonics* **2** 175

[18] Qiaoqiang Gan, Zhan Fu, Ding Yujie and Bartoli Filbert J 2008 *Phys. Rev. Lett.* **100** 256803

[19] Liu J S, Ding L, Wang K J and Yao J Q 2009 *Opt. Express* **17** 12714

[20] Taflove A and Hagness S C 2000 *Computational Electrodynamics: The Finite-Difference Time-Domain Method* 2nd. edn (Boston: Artech House)

[21] Zhang Fu, Qiaoqiang Gan, Ding Yujie and Bartoli Filbert J 2008 *IEEE Journal of Selected Topics in Quantum Electronics* **14** 486

[22] Weiner J 2009 *Rep. Prog. Phys.* **72** 1

[23] Bora Ung and Yunlong Sheng 2007 *Opt. Express* **15** 1182